Nonlinear Coherent Transport Through Doped Nanotube Junctions

Amir A. Farajian, Keivan Esfarjani, and Yoshiyuki Kawazoe
Institute for Materials Research, Tohoku University, Sendai 980-8577, Japan
(Received 30 October 1998; revised manuscript received 9 February 1999)

The electronic and phase-coherent transport properties of doped carbon nanotube junctions are studied. It is shown that there are regions of negative differential resistance in the I-V characteristic of small radius metallic tubes, which are not seen for semiconducting tubes. Their origin, as discussed, is different from that of traditional Esaki diodes and resonant tunneling structures. Semiconducting tube characteristics, however, show a region of zero current for nonzero voltages which is asymmetric with respect to the applied bias if there is different doping on each side of the junction. [S0031-9007(99)09542-3]

PACS numbers: 72.80.Rj, 73.23.–b, 73.40.Ei

The possibility of doping carbon nanotubes with alkali or halogen atoms has been the subject of recent experiments [1,2] and theoretical works [3]. It has been shown experimentally that introducing dopants changes the conductivity of nanotubes [2,4]. An *ab initio* method based on the all electron density functional formalism has been used to study the feasibility of inserting typical alkali metals into nanotubes [5]. Nanotube doping can also be achieved through interaction with a substrate, which affects the carrier concentration and shifts the chemical potential of the tube [6]. On the other hand, it is now understood that electronic properties of nanotubes strongly depend on their geometry. This geometry is usually specified by a pair of integers (m, n) [7].

It is the purpose of the present work to study the nonlinear transport characteristics of doped nanotube junctions. These junctions are formed by shifting the levels of each half of the tube, in the absence of bias, through doping. The overall shift of the energy levels can result from different ways of doping the two sides of the tube and/or applying an external potential difference between them. Two sides of a nanotube can have different dopings due to the introduction of different dopant atoms [8]. Substrate doping can also be different for two sides of a nanotube due to, for example, polycrystal substrate or substrate roughness. For the case of doping by the substrate, a typical experimental value of the initial shift of the chemical potential as a result of doping is ~ 0.3 eV [6] for Au substrate, which is due to the difference of the work functions of the nanotube and the substrate. For doping by typical alkali and halogen atoms, on the other hand, the initial shifts were found to be ~ -0.5 and ~ 0.5 eV, respectively, by a previous 4-orbital/atom self-consistent tight-binding calculation of ours [8].

In order to calculate electronic and transport properties of doped nanotube junctions, we exploit the self-consistent tight-binding approach [9] to properly include the effects of charge transfer at the junction. The surface Green's function matching (SGFM) method [10] is then used to obtain the transmission matrices. Finally, Landauer's formalism is used to obtain the conductance and the current-voltage (I-V) characteristic of the system. The present study is restricted to phase-coherent transport; i.e., the electron-phonon interaction is ignored.

Within the self-consistent tight-binding formalism, we model a carbon nanotube by the following Hamiltonian:

$$H = \sum_i (\varepsilon_i + U_H \delta n_i) a_i^\dagger a_i + \sum_{\langle ii' \rangle} V_\pi a_i^\dagger a_{i'}, \qquad (1)$$

where the sum over lattice sites i and i' is restricted to nearest neighbors. We consider one π orbital per atom and set the value of the hopping integral equal to 1. (Experiments [6] show good agreement with theoretical results for $V_\pi = 2.7 \pm 0.1$ eV.) Henceforth, the unit of energy is chosen to be the hopping integral, unless otherwise specified. The Hubbard term $U_H \delta n_i$ is added for the self-consistent treatment of charge transfer at the junction, and δn_i is the change in the occupation number at site i, compared to that of the bulk crystal. The self-consistent treatment is needed in order to obtain the exact form of the potential drop at the junction, especially when a large external potential difference is applied to the two sides of the system. We use the experimental value of the Hubbard coefficient U_H for carbon, $U_H = 10.00$ eV [11], which is nearly 4 times the hopping integral (we set $U_H = 4$).

We consider two such systems, call them A and B, and attach them together at the junction. Each system (nanotube) is a semi-infinite quasi-one-dimensional lattice, which can be divided into successive identical principal layers. A principal layer is composed of a few unit cells of the crystal under consideration such that each principal layer interacts only with its nearest neighbors. In the present study, on-site energies ε_i of the system A are considered to be $V + U_{0A}$. They are shifted compared to those of the system B, taken to be U_{0B}. Here, U_{0A} and U_{0B} indicate the initial shifts of the chemical potentials of systems A and B due to doping, and V is the external potential difference applied to the two sides of the system. Therefore, in computing transport properties, the applied bias V enters as a parameter in the scattering matrix and the transmission matrix elements. In other words, the scattering matrix would be a functional of the (self-consistent)

 0031-9007/99/82(25)/5084(4)$15.00

potential drop profile at the junction, which itself depends on the applied bias V. This approach is analogous to the one adopted in recent studies [12] on transport in coherent mesoscopic systems in order to include the nonlinear effects. As an example to illustrate the effect of doping, in the present work initial shifts $U_{0A} = 0.2$ and $U_{0B} = 0.1$, and $U_{0A} = 0.3$ and $U_{0B} = 0.0$, are assumed in the calculations for metallic and semiconducting tubes, respectively. These values determine the initial position of chemical potentials with respect to the density of states when there is no external bias.

The potential drop profile at the junction is depicted in Fig. 1 for $V = 0.5$ and $V = 2$, in the $(3,0)$ metallic zigzag tube and in the $(7,0)$ semiconducting zigzag tube. In this figure, each layer index indicates a ring of carbon atoms, which consists of 3 and 7 atoms in the $(3,0)$ and $(7,0)$ tubes, respectively. Layers 1 through 4 indicate the rings of the last principal layer of system B, while layers 5 through 8 indicate the rings of the first principal layer of system A. These two principal layers define the interface region. Without the self-consistent treatment, the potential drop profile at the junction would be a step of height 0.5 for $V = 0.5$, and of height 2 for $V = 2$. Self-consistent calculation, however, results in deviation from the step drop, and smoothens the potential profile. We can notice small oscillations for larger biases. As we have assumed that the potential drop occurs only within the interface region, the electric field is fully screened in this region and the total charge of the junction is conserved.

There are different approaches to calculate transmission matrix elements [13] for the matched system. Following Chico *et al.* [14], we calculate these elements using the SGFM method. The conductance of the system is then obtained from Landauer's formula [15] as $\Gamma(E,V) = (2e^2/h)T(E,V) = (2e^2/h)\sum_{\alpha\beta}|t_{\alpha\beta}|^2$, where $t_{\alpha\beta}$ is the transmission matrix element between channels α of system A and β of system B, and $T(E,V)$ is the transmission coefficient between A and B. Finally, the current across the junction is obtained using the Landauer-Büttiker formula [16]

$$I(V) = \frac{2e}{\hbar}\int_{-\infty}^{\infty} dE\, T(E,V)[f_B(E) - f_A(E)], \qquad (2)$$

where f_A and f_B are the Fermi distributions of systems A and B, respectively.

The results of conductance calculations are shown in Fig. 2(a) for the junctions in a $(4,4)$ armchair tube, and in Fig. 2(b) for a $(7,0)$ zigzag tube, for different values of the bias V. These tubes have nearly equal radii; 2.67 Å for $(4,4)$ and 2.70 Å for $(7,0)$. In these calculations, both sides of the junction have the same geometry; i.e., both are either armchair or zigzag. Figure 2 shows that by shifting the chemical potential of one side of the system, both the number of conducting channels and the transmission coefficient are changed compared to the $V = 0$ case. In order to describe the effect of decrease and/or increase of the number of conducting channels for each energy and the selection rule involved, we consider, as an example, the band structure of the $(4,4)$ tube, which is depicted in Fig. 3(a). The armchair tube $(4,4)$ has fourfold rotational symmetry; therefore the states in each of the nondegenerate bands in Fig. 3(a) are eigenstates of the rotation operator around the axis of the tube, with the same eigenvalue. Degenerate bands, however, are linear combinations of the eigenstates of the rotation operator whose eigenvalues can

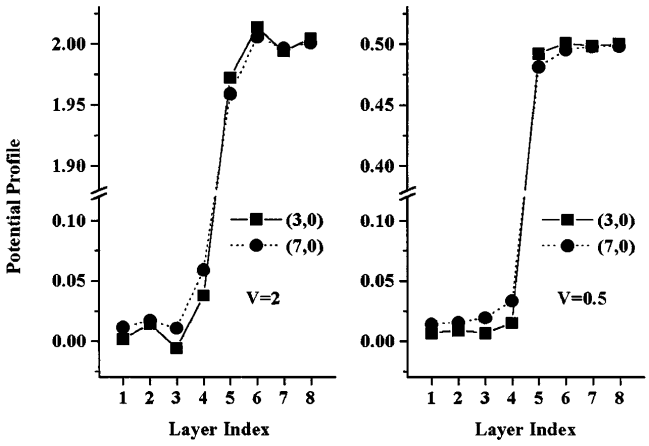

FIG. 1. Self-consistent potential drop at the junction.

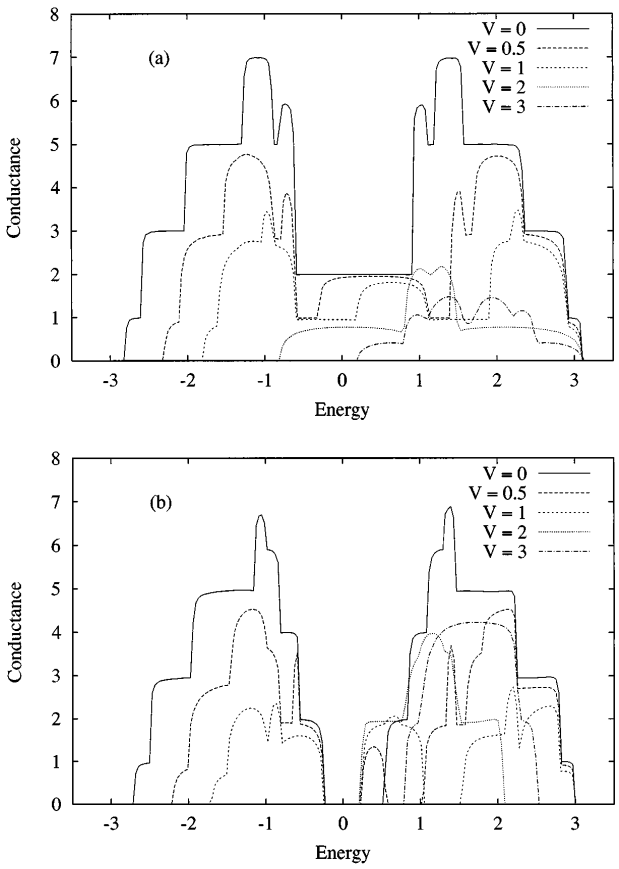

FIG. 2. Conductance of doped nanotube junctions (in units of $2e^2/h$) for different values of the potential difference V for (a) armchair tube $(4,4)$, and (b) zigzag tube $(7,0)$. All energies are in units of the hopping integral.

be extracted by diagonalizing the rotation operator within the degenerate subspace. In Fig. 3(a), all the bands are double degenerate except for the uppermost and lowermost ones, as well as the two bands crossing at the Fermi level. The bands are labeled according to their eigenvalue under rotation, $\exp(im\pi/2)$; $m = 0, 1, 2, 3$. Consider the conductance of the $(4,4)$ tube for $V = 0$ as an example. Figure 3(a) shows that at $E = -0.5$ there are only two conducting channels with positive group velocities and with the same rotational eigenvalue 1, in each of the systems A and B. Therefore at this energy the conductance of the unbiased tube is $2 \times 2e^2/h$. Now consider the case of a biased tube with $V = 1$. The band structure of medium A would be shifted along the energy axis by one unit, and is depicted in Fig. 3(b). At $E = -0.5$, the two channels which were conducting for $V = 0$ are not conducting for $V = 1$. Instead, only one channel with rotational eigenvalue 1 and positive group velocity is now conducting, namely, in the lowermost band in Fig. 3(b). Therefore, one of the conduction channels is suppressed and the conductance is decreased by one unit. Moreover, the overall rounding of conductance curves, which produces further reduction of conductance, results from imperfect conduction ($|t_{\alpha\beta}|^2 < 1$) between channels with the same rotational eigenvalue, but different wave vectors.

The I-V characteristics at temperature $T = 0$ of $(4,4)$ and $(3,3)$ armchair tubes, as well as those of $(7,0)$, $(5,0)$, and $(3,0)$ zigzag tubes, are depicted in Figs. 4(a) and 4(b). These curves are obtained by assuming a step potential difference at the junction, without any self-consistent calculation of the potential drop. For the $(3,0)$ tube, however, the curve obtained from a self-consistent treatment is also given for comparison. One can notice that the current from the self-consistent calculation is larger than the current of the step potential calculation. As is apparent from Fig. 1, the smoothening effect of the self-consistent treatment of the $(3,0)$ tube is of the same order as that of a larger tube $(7,0)$. Therefore, we expect that the self-consistent calculations of the current for larger tubes also differ slightly from the step potential ones.

It is seen from Fig. 4(a) that for the armchair case, there are regions of negative differential resistance (NDR), starting at $|V| \simeq 1$ (the exact value depends on the initial dopings). This occurs when the conductance reduced by the suppression of one conduction channel enters the integration window $f_B(E) - f_A(E)$ in Eq. (2) [as is explicitly seen from Fig. 2(a)]. As $|V|$ is further increased, this reduction of current persists until the shift of the Fermi level of medium A causes other channels with the same rotational eigenvalue to conduct, so that the current begins to increase again. This occurs at $|V| \simeq 1.40$ for the $(4,4)$ tube, and at $|V| \simeq 1.68$ for the $(3,3)$ tube. These are the widths of the (pseudo)gap of these metallic tubes. We can notice an enhancement of the NDR as the tube radius gets smaller. The NDR feature has a wide range of applications including amplification, logic, and memory, as well as fast switching. The unique character of the NDR of metallic nanotubes is that its mechanism, i.e., the selection rule involved, is a direct consequence of the rotational symmetry of carbon nanotubes, and is different from the mechanism responsible for NDR in Esaki diodes and resonant tunneling structures. As the main cause of NDR is the

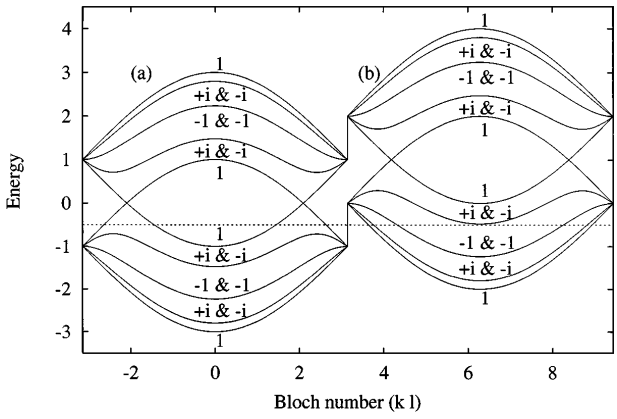

FIG. 3. Band structure of the $(4,4)$ armchair tube for (a) $V = 0$ and (b) $V = 1$. For the horizontal axis, l is the lattice constant between two adjacent principal layers. Band labels indicate rotational eigenvalues.

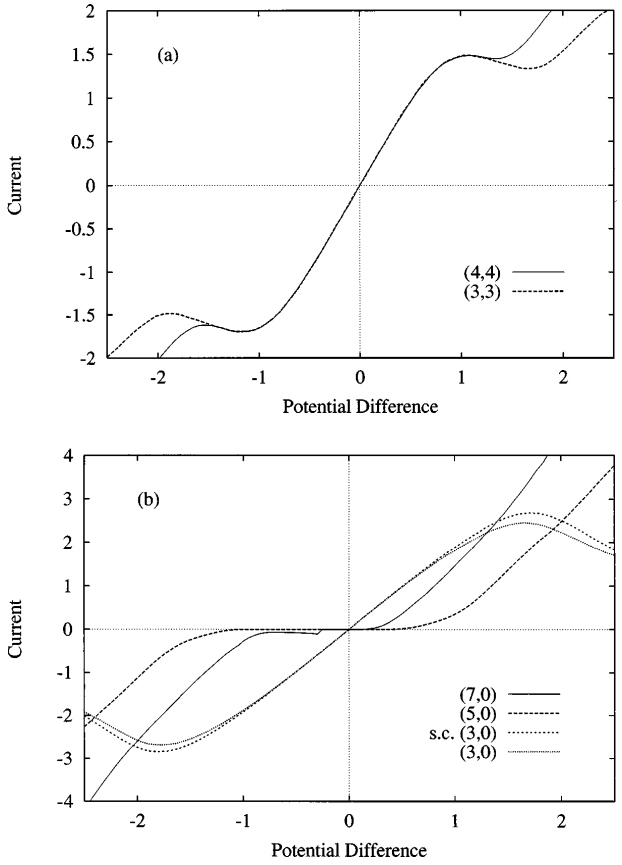

FIG. 4. Current (in units of hopping $\times 2e/\hbar$) for (a) armchair tubes $(4,4)$ and $(3,3)$, as well as (b) zigzag tubes $(7,0)$, $(5,0)$, and $(3,0)$. For the $(3,0)$ tube, the self-consistent (s.c.) solution is also given for comparison.

rotational symmetry selection rule between the eigenstates of bulk systems A and B, we do not expect the assumption of sharp potential drop to qualitatively modify the results of our calculations.

Next we consider the case of zigzag tubes in Fig. 4(b). While there exist regions of NDR for the $(3,0)$ metallic zigzag tube, the I-V characteristics of $(7,0)$ and $(5,0)$ semiconducting zigzag tubes do not contain regions of NDR. However, there exists a region of zero current for nonzero potential differences in the I-V characteristic of these semiconducting tubes, which is asymmetric with respect to the sign of the bias. This arises from the asymmetric modification of the gap of these tubes due to the initial dopings. The small leakage current which is observed for the $(7,0)$ tube is due to the fact that for this tube the maximum conduction condition, $V = -|U_{0A} - U_{0B}| = -0.3$, occurs out of the gap. Because of the asymmetry of its I-V characteristic, the junction of doped semiconducting tubes can function as a rectifier, in much the same way that an ordinary p-n junction is used for rectification, provided that $|U_{0A} - U_{0B}|$ is large enough.

A few comments are now in order. First, the above mentioned effects for metallic and semiconducting nanotubes depend on the detail of their band structure, i.e., the width of the gap and the interband separation for eigenstates with different rotational eigenvalues. As the gap width is inversely proportional to the diameter of the tube [7] and the number of bands increases with increasing diameter, we expect these effects to diminish for tubes with larger diameters. Second, temperature affects transport through both the Fermi distributions of electrons in Eq. (2) and the electron-phonon interactions. The former effect is negligible unless at temperatures comparable to the hopping integral. As for the effect of phonons, one can assume that only acoustic phonons can scatter electrons, provided that the temperature is below the optical phonon frequency. Acoustic phonons only slightly modify the hopping integrals due to small lattice distortions. For the metallic and semiconducting tubes, because of having few and no states at the Fermi level, respectively, and given the very low energy of phonons, they cannot scatter electrons from an occupied state to an empty state except at the interface region, which is a negligible volume of the whole system. We therefore expect the electron-phonon interaction to be negligible, especially for $kT < \hbar\omega_{\text{optic}}$. Third, up to now, it was assumed that the rotational symmetry of the tube is not broken as a consequence of doping. In real situations, however, it might not be the case. Donor and/or acceptor dopants might be located closer to some of the carbon atoms than others, and the effect of substrate doping depends on the distance from the substrate. We have investigated the effect of small disorders, either static or due to phonons, by adding random numbers of mean zero and standard deviation 0.05 to the on-site energies. It was found that the current decreased by $\sim 10\%$. The qualitative features of the I-V curves, however, were not affected. Fourth, the phenomena predicted here can be observed in experiments, provided that the nanotube diameters are small enough. The substrates for the two sides of the junction should have the same height in order to prevent the formation of bending defects [17], or additional inhomogeneities. Moreover, the experiments should be performed at sufficiently low temperatures in order to prevent the incoherency caused by electron-phonon interactions.

In conclusion, the nonlinear I-V characteristics of doped metallic and semiconducting nanotube junctions are calculated. It is shown that suppression of one conduction channel, due to the rotational symmetry selection rule, results in regions of negative differential resistance (NDR) for metallic tubes. For semiconducting tubes, on the other hand, a rectifying characteristic is observed due to the different initial dopings. The above mentioned effects depend on the details of the band structure and are diminished for tubes with larger diameters.

The authors thank Dr. L. Chico, Professor M. Sluiter, and N. Taghavinia for fruitful comments.

[1] O. Stephan *et al.,* Science **266**, 1683 (1994).
[2] L. Grigorian *et al.,* Phys. Rev. B **58**, 4195 (1998).
[3] Y. Miyamoto *et al.,* Phys. Rev. Lett. **74**, 2993 (1995).
[4] R. S. Lee *et al.,* Nature (London) **388**, 255 (1997).
[5] A. A. Farajian *et al.,* J. Chem. Phys. (to be published).
[6] J. W. G. Wildoer *et al.,* Nature (London) **391**, 59 (1998); S. J. Tans *et al.,* Nature (London) **386**, 474 (1997); M. Bockrath *et al.,* Science **275**, 1922 (1997); S. J. Tans *et al.,* Nature (London) **393**, 49 (1998).
[7] M. S. Dresselhaus *et al., Science of Fullerenes and Carbon Nanotubes* (Academic Press, New York, 1996).
[8] K. Esfarjani *et al.,* Appl. Phys. Lett. **74**, 79 (1999).
[9] K. Esfarjani and Y. Kawazoe, J. Phys. Condens. Matter **10**, 8257 (1998).
[10] M. C. Munoz *et al.,* Prog. Surf. Sci. **26**, 117 (1988); F. Garcia-Moliner and V. R. Velasco, *Theory of Single and Multiple Interfaces* (World Scientific, Singapore, 1992).
[11] R. G. Pearson, Inorg. Chem. **27**, 734 (1988).
[12] M. Büttiker, J. Phys. Condens. Matter **5**, 9361 (1993); T. Christen and M. Büttiker, Europhys. Lett. **35**, 523 (1996).
[13] M. P. Anantram and T. R. Govindan, Phys. Rev. B **58**, 4882 (1998); J. Cserti *et al.,* Phys. Rev. B **57**, 15 092 (1998); R. Tamura and M. Tsukada, Phys. Rev. B **55**, 4991 (1997); **58**, 8120 (1998).
[14] L. Chico *et al.,* Phys. Rev. B **54**, 2600 (1996); Phys. Rev. Lett. **81**, 1278 (1998).
[15] D. S. Fisher and P. A. Lee, Phys. Rev. B **23**, 6851 (1981).
[16] M. Büttiker *et al.,* Phys. Rev. B **31**, 6207 (1985).
[17] A. Bezryadin *et al.,* Phys. Rev. Lett. **80**, 4036 (1998).